Electronic Supplementary Material (ESI) for Soft Matter.

ELECTRONIC SUPPLEMENTARY MATERIAL

Synchronized oscillations, traveling waves, and jammed clusters induced by steric interactions in active filament arrays

Raghunath Chelakkot[1], Michael F. Hagan[2], and Arvind Gopinath[3]

[1]*Department of Physics,*

Indian Institute of Technology Bombay,

Mumbai 400076, India

[2]*Martin A. Fisher School of Physics,*

Brandeis University, Waltham, MA, USA.

[3]*Department of Bioengineering,*

University of California, Merced, CA, USA

I. TWO FILAMENT SYSTEMS

The geometry of the two filament case is as follows. We clamp (the bases of) two filaments at a fixed separatation Δ along the x axis (Figure 1(a) in the main text, so that the parameter $\delta = (\Delta - \sigma)/\ell_0$. Since the dynamics of a single isolated filament is completely determined (In our setting) by the activity number β, we compare the oscillatory dynamics of the filaments for three values, $\beta = 768$, 384, and 192. The dimensionless frequencies and maximum amplitudes in the absence of interactions ($\mathcal{A}_{\max}$) are listed for these values of β in Table 2 of the main text.

When the inter-filament separation is much larger than the oscillation amplitude in the x direction, $\delta \gg \mathcal{A}_{\max}$, the filament interaction is zero, and we recover the oscillatory pattern for isolated filaments. Therefore, we focus on the range $1 \leq \delta \leq \mathcal{A}_{\max}$. Based on the simulation results, we broadly classify the collective oscillations into three categories as follows.

First, when $\delta \simeq 1$ and for all β greater than the critical value for the onset of oscillations, we find that contact interactions qualitatively modify filament oscillations, reshaping the waveform with an additional minimum emerging in L_{ee}(Fig. S1(a)). Moreover, there is a constant phase shift between oscillations of the two filaments. Next, we measure the trajectory of the free ends of both the filaments (Fig S1(b)). Unlike for isolated filaments, the end-segment trajectory shows an asymmetric pattern, with oscillations skewed in the direction away from the neighboring filament. Steric interactions hinder bending toward the neighbor and promote bending away from it. This mechanism also explains the appearance of the second minimum in L_{ee}, which arises due to the occluded bending of the filament in one direction, reducing its maximal end-to-end length. In Fig. S1(c), we plot the time-derivative of the x component of the end-segment position, dX/dt, (X being the x value of the filament tips); these trajectories follow noisy, symmetric, closed loops for both filaments. For comparison, we show the result with thermal noise turned off in the simulations, which corresponds to smooth closed trajectories.

Increasing the inter-filament spacing qualitatively changes the form of L_{ee} (Fig. S1(d)), with a significant reduction in one of the minima of the peak-to-peak oscillation compared to Fig. S1(a). Analyzing the free-end trajectory (Fig. S1(e)) shows that one of the filaments (which one is stochastic due to the left-right symmetry of the initial non-oscillating state)

gets jammed under its neighbor. Thus, the oscillatory pattern of the jammed filament gets qualitatively modified while the 'dominant' filament oscillates with a higher amplitude that its neighbor. This behaviour is most prominent around $\delta \simeq \mathcal{A}_{\max}/2$. This asymmetry in interaction also affects the periodic nature of $L_{\rm ee}$, especially for the jammed filament. On the other hand, the dX/dt vs X dependence resembles that of the closely spaced filaments (Fig S1(f)).

Further increase in the inter-filament spacing to values $\delta \simeq \delta_{\max}$ reduces typical contact durations, with symmetry arguments suggesting that contact occurs in the same region for either filament. Consequently, we observe statistically similar waveforms and oscillations for both filaments (Fig. S1(g)). Trajectories of the free ends for both filaments overlap (Fig. S1(h)), indicating a non-vanishing contact.

For filaments with smaller activity (smaller value of the active force densities) or higher rigidity, ($\beta = 192$), we find that the jamming behaviour is absent. Although the interaction significantly alters the waveform in $L_{\rm ee}$ and distorts synchronization between the filaments, the effect is equal for both the filaments as neither of the filaments becomes continually jammed. At a larger separation $\delta \simeq \delta_{\max}$ the periodic forcing acting on either filament combined with the activity results in a reemergence of synchronization, with this effect being more prominent for filaments with lower activity number ($\beta = 192$), where the $L_{\rm ee}$ waveforms of the two filaments exhibit near perfect overlap.

With high activity number and intermediate inter-filament spacing, the two filaments exhibit different oscillatory patterns because one filament dominates and restricts the oscillations of its neighbor. In contrast, for smaller activity number the inter-filament interaction leads to a similar oscillatory pattern in both the filaments with a constant phase difference.

II. THREE FILAMENT SYSTEMS

In an array of three filaments, the collective oscillatory pattern depends on the filament softness (via the activity number β). Similar to the two-filament system, the soft filaments ($\beta = 768$) show maximum deformation and the oscillatory patterns are different for all the three filaments (Fig S2(a)). However, for an array of stiffer filaments ($\beta = 384, 192$) the oscillatory pattern of the middle filament is different from both the end-filaments. At large separation, $\delta \gtrsim \delta_{\max}$ the neighboring filaments do not interact continuously, hence the

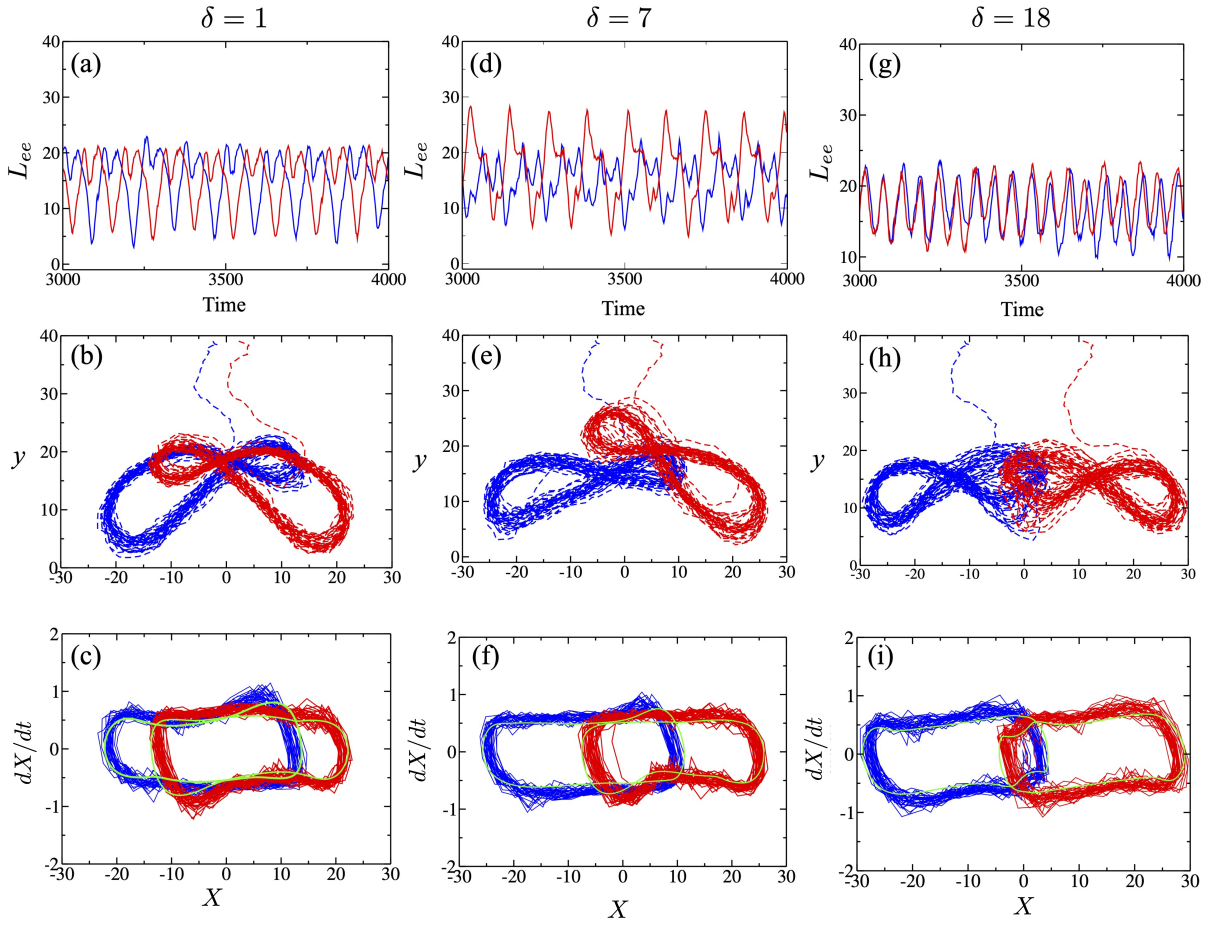

FIG. S1. Dynamics of two clamped filaments. The length of the end-end vector $L_{\rm ee}$, the trajectory of the free end in the $x-y$ plane, and the tip velocity, dX/dt, with X being the x component of the tip (free end), are plotted as a function of time for a system with $N = 2$ and $\beta = 384$. We show (a,b,c) a relatively close pair ($\delta = 1$), (d,e,f) intermediate packing ($\delta = 7$) and (g,h,i) loose packing ($\delta = 18$); here $\delta_{\rm max} = 12.5$. The green curves in (c,f,i) refer to the results for a simulation in the absence of thermal noise. Results are shown for smooth filaments with $\sigma/\ell_0 = 4$. Comparing the green and the red/blue data points, we see that in this instance, the perturbation due to noise is weak.

deformation caused by it is minimal. At this separation, we observe a reemergence of synchronization between the filaments. This synchronization at large separation is particularly strong for stiffer filaments (Fig S3).

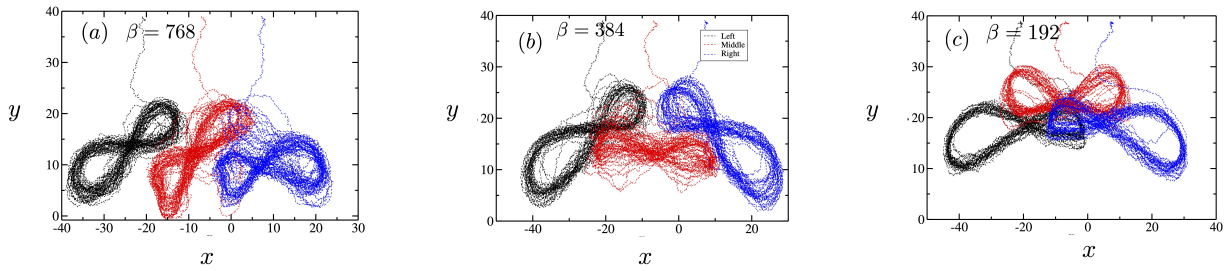

FIG. S2. The end-segment trajectory in $x-y$ space of three filament system, at intermediate separation ($\delta = 10$). The collective oscillatory pattern is different for different filament stiffness, (a) $\beta = 768$ (b) $\beta = 384$, and (c) $\beta = 192$. The softer filaments characterized by elasticity parameters $\beta = 768$ and 384 display maximum deformation; stiffening the filaments alters their oscillatory patterns in response to the contact forces.

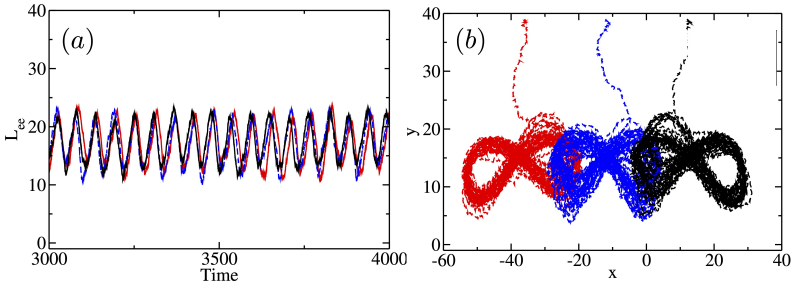

FIG. S3. (a) The end-end length L_{ee} time-series and (b) the end-segment trajectory in $x-y$ space of three filaments with $\beta = 192$ and separation, $\delta = 19$ ($\delta_{\max} = 17.5$).